

Non-Maxwellianity of Ion Velocity Distributions in the Earth's Magnetosheath

Louis Richard,^{1,2,*} Sergio Servidio,³ Ida Svenningsson,^{1,4} Anton V. Artemyev,²
Kristopher G. Klein,⁵ Emiliya Yordanova,¹ Alexandros Chasapis,⁶ and Oreste Pezzi⁷

¹Swedish Institute of Space Physics, Uppsala 751 21, Sweden

²Department of Earth, Planetary, and Space Sciences,
University of California, Los Angeles, California 90095, USA

³Università della Calabria, Arcavacata di Rende, 87036, IT

⁴Department of Physics and Astronomy, Uppsala University, Uppsala 751 20, Sweden

⁵Lunar and Planetary Laboratory, University of Arizona, Tucson, AZ, USA

⁶Laboratory for Atmospheric and Space Physics, University of Colorado, Boulder, Colorado 80303, USA

⁷Istituto per la Scienza e Tecnologia dei Plasmi,

Consiglio Nazionale delle Ricerche (ISTP-CNR), 70126 Bari, Italy

(Dated: April 9, 2025)

We analyze the ion velocity distribution function (iVDF) deviations from local thermodynamic equilibrium (LTE) in collisionless plasma turbulence. Using data from the Magnetospheric Multiscale (MMS) mission, we examine the non-Maxwellianity of 441,577 iVDFs in the Earth's magnetosheath. We find that the iVDFs' anisotropy is overall limited, while high-order non-LTE features can be significant. Our results show that the complexity of the iVDFs is strongly influenced by the ion plasma beta and the turbulence intensity, with high-order non-LTE features emerging with large-amplitude magnetic field fluctuations. Furthermore, our analysis indicates that turbulence-driven magnetic curvature contributes to the isotropization of the iVDFs by scattering the ions, emphasizing the complex interaction between turbulence and the velocity distribution of charged particles in collisionless plasmas.

Introduction - Inter-particle Coulomb collisions are nearly negligible in most astrophysical plasma environments, such as accretion disks, the intracluster medium, and the heliosphere [1, 2]. Consequently, the velocity distribution functions of charged particles can significantly deviate from the local thermodynamic equilibrium (LTE) Maxwell-Boltzmann distribution [3]. *In situ* observations and numerical simulations have shown that complex non-Maxwellian ion velocity distribution functions (iVDFs) are characteristic of collisionless plasma processes, including magnetic reconnection [4, 5], turbulence [6–9], Kelvin-Helmholtz instabilities [10], and shocks [11, 12]. These non-Maxwellian iVDFs serve as a reservoir of free energy, driving kinetic velocity-space plasma instabilities that relax the system toward a marginally stable equilibrium through, e.g., Landau/cyclotron resonant diffusion [3]. For example, *in situ* observations suggest that anisotropic, non-LTE iVDFs excite electromagnetic waves, which in turn modify the distributions via resonant ion-cyclotron interactions [13–15]. Understanding the complexity of iVDFs is therefore essential for investigating non-Maxwellian equilibria's stability and the energy conversion and dissipation mechanisms in collisionless plasmas [16].

In situ observations in the solar wind and the Earth's magnetosheath indicate that departures of iVDFs from LTE are constrained by the growth of temperature anisotropy-driven mirror, ion-cyclotron, and firehose instabilities [13, 17]. However, the traditional approach to studying plasma stability using linear and quasi-linear Vlasov theory with bi-Maxwellian ions presents two key limitations. First, more complex “high-order”

non-Maxwellian features, such as agyrotropy and ion beams — arising from processes like population mixing — can also excite electromagnetic and electrostatic modes, contributing to plasma heating [3, 18–20]. Second, linear and quasi-linear Vlasov theory assumes small-amplitude perturbations around the background magnetic field \mathbf{B}_0 [3]. This assumption may be limited in highly turbulent environments such as the solar wind and planetary magnetosheaths [21]. Furthermore, recent studies suggest that pitch-angle scattering in kinetic-scale discontinuities and Alfvénic current filaments and flow vortices may supplement or even surpass cyclotron resonant diffusion in isotropizing iVDFs [5, 22–24]. Thus, the nature of fundamental processes relaxing the iVDFs toward LTE and heating collisionless plasmas remains unclear.

Data - In this Letter, we use *in situ* observations to investigate the non-Maxwellianity of iVDFs in turbulent space plasma. We analyze data from the Magnetospheric Multiscale (MMS) spacecraft in Earth's magnetosheath — a region of shocked, newly generated turbulent plasma where magnetic reconnection is frequently observed [25–28]. We focus on a subset of the dataset from Ref. [29], limiting to intervals where the spacecraft separation is smaller than the ion inertial length $d_i = \sqrt{m_i/\mu_0 n_i e^2}$, with n_i the ion number density. Additionally, we require that the tetrahedral configuration quality ensures a gradient estimation error of $\lesssim 10\%$ [30]. This selection results in 18.4 hours of data, corresponding to 441,577 iVDFs, with a cadence of 150 ms $\simeq 0.04 f_{ci}^{-1}$, where $f_{ci} = \omega_{ci}/2\pi = eB/2\pi m_i$ is the ion cyclotron frequency,

with $B = |\mathbf{B}|$ denoting the magnetic field strength. We use magnetic field measurements from the fluxgate magnetometer instrument [31] and iVDFs and their moments from the fast plasma investigation instrument [32]. We correct the ion data for penetrating radiation effects and spacecraft spin tones [33] and average across the four MMS spacecraft to improve counting statistics and minimize uncertainties.

Results - We investigate the non-Maxwellianity of the iVDFs in the $(\beta_{i\parallel}, T_{i\perp}/T_{i\parallel})$ parameter space, where $T_{i\perp(\parallel)}$ denotes the ion temperature perpendicular (parallel) to the local magnetic field $\hat{\mathbf{b}} = \mathbf{B}/B$, and $\beta_{i\parallel} = 2\mu_0 n_i k_B T_{i\parallel}/B^2$ is the parallel ion plasma beta. While this approach is commonly adopted, we will later show its limitations. Fig. 1(a) shows the joint probability density function (PDF). We find that the majority (68%) of the iVDFs lie within the stability limits predicted by linear Vlasov theory. In particular, the perpendicular temperature anisotropy $T_{i\perp}/T_{i\parallel} > 1$ is well constrained by the threshold associated with a mirror-mode instability growth rate of $\gamma/\omega_{ci} = 10^{-2}$ (red dashed line), consistent with previous observations [17]. However, 32% of iVDFs fall outside these stability limits, indicating that unstable iVDFs are frequently observed.

To further quantify deviations from LTE, we now examine the agyrotropy of the iVDFs. We use Swisdak's agyrotropy parameter, defined as [34]:

$$\sqrt{Q_i} = \sqrt{\frac{p_{i12}^2 + p_{i13}^2 + p_{i23}^2}{p_{i\perp}^2 + 2p_{i\perp}p_{i\parallel}}}, \quad (1)$$

where $\sqrt{Q_i} \in [0, 1]$, with $\sqrt{Q_i} = 0$ for a perfectly gyrotropic iVDF. Here, $p_{i\perp(\parallel)}$ denotes the ion pressure perpendicular (parallel) to the local magnetic field $\hat{\mathbf{b}}$, and p_{i12} , p_{i13} , and p_{i23} are the off-diagonal components of the pressure tensor in a reference frame rotated around $\hat{\mathbf{b}}$. We find that the agyrotropy is generally very small, with $\sqrt{Q_i} = 0.04^{+0.02}_{-0.02}$ [Fig. 1(b)]. However, 4% of the iVDFs exhibit significant agyrotropy with $\sqrt{Q_i} \gtrsim 0.1$, which is typically observed in current sheets and magnetic reconnection regions [35]. This result indicates that the iVDFs are predominantly gyrotropic on average, with only rare extreme agyrotropy typically occurring in intervals exceeding stability conditions.

To capture the more complex non-LTE features — such as beams or other non-thermal features — we investigate the higher-order non-Maxwellianity of the iVDFs. We adopt the normalized L^1 norm of the non-Maxwellian phase-space density residue, defined by Ref. [38] as:

$$\varepsilon_i = \frac{1}{2n_i} \int_{v_{min}}^{v_{max}} |f_i - f_{i\text{bM}}| d^3v, \quad (2)$$

where $\varepsilon_i \in [0, 1]$. Here, f_i is the measured iVDF, and

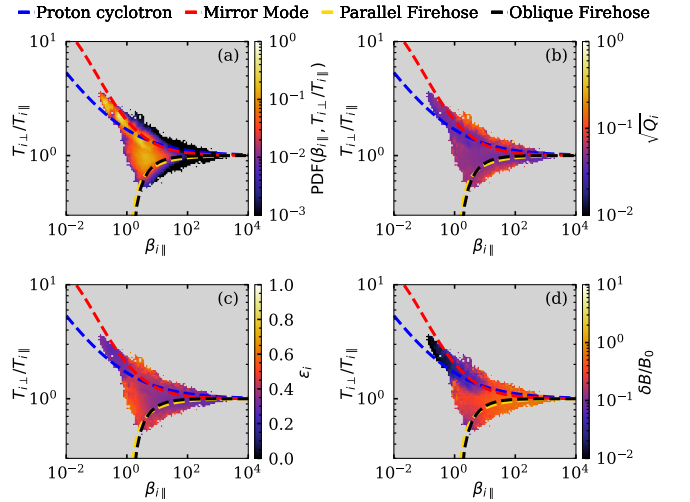


FIG. 1. Non-Maxwellianity of iVDFs relative to the magnetic field. (a) Joint PDF of $T_{i\perp}/T_{i\parallel}$ and $\beta_{i\parallel}$. (b)–(d) Conditional averages of the agyrotropy $\sqrt{Q_i}$, non-bi-Maxwellianity ε_i , and magnetic fluctuation amplitude $\delta B/B_0$ at $k\rho_i \simeq 1$. Dashed lines mark instability thresholds for $\gamma/\omega_{ci} = 10^{-2}$ from Ref. [36]. Bins with fewer than nine counts are omitted due to Poisson errors [37].

$f_{i\text{bM}}$ is the bi-Maxwellian distribution with the same bulk moments (density, bulk velocity, and temperature anisotropy) as f_i . The integral is evaluated within an energy range where the phase-space density is at least 1σ above the penetrating radiation model [33] and the noise floor (one count level). Typically, this corresponds to $v_{min} \simeq 0.5v_{thi}$ and $v_{max} \simeq 6.8v_{thi}$, where $v_{thi} = \sqrt{2k_B T_i/m_i}$ denotes the ion thermal speed. We find that the non-bi-Maxwellianity is overall moderate, with $\varepsilon_i = 0.36^{+0.11}_{-0.07}$ [Fig. 1(c)]. We note that the magnitude of ε_i may be systematically offset due to the finite grid resolution [5]. The non-bi-Maxwellianity remains small near marginal stability ($\varepsilon_i \simeq 0.29$) but increases away from the stability limits. Significant deviations from bi-Maxwellian LTE emerge on both sides of the theoretical stability boundaries, with ε_i reaching $\simeq 0.90$. This indicates that iVDFs can have substantial high-order non-bi-Maxwellian features even at moderate anisotropy.

We now investigate magnetic field fluctuations associated with iVDFs, focusing on ion-scale fluctuations at $k\rho_i \simeq 1$, where $\rho_i = v_{thi\perp}/\omega_{ci}$ is the ion Larmor radius. We assume a power-law decay in the power spectral density and apply Taylor's hypothesis, which holds since the ion bulk speed V_i satisfies $V_i \simeq 4V_A > V_A$. Here, $V_A = B_0/\sqrt{\mu_0 n_i m_i}$ is the Alfvén speed, and $B_0 = |\langle \mathbf{B} \rangle_{30s}|$ is the background magnetic field, where $\langle \cdot \rangle_{30s}$ represents a 30-second average. We choose the averaging window to span several ($\sim 3-10$) correlation lengths λ_c [28, 29]. We compute the normalized magnetic field wave amplitude $\delta B/B_0$, using a high-pass filter with a cutoff frequency corresponding to $k\rho_i \simeq 1$, meaning $f \geq \langle V_i \rangle_{30s}/2\pi \langle \rho_i \rangle_{30s}$.

For $\beta_{i\parallel} < 1$ and $T_{i\perp}/T_{i\parallel} > 1$, near marginal stability [Fig. 1(a)], we find that the magnetic fluctuation amplitude is $\delta B/B_0 \sim 10^{-2}$ [Fig. 1(d)]. In contrast, for $\beta_{i\parallel} > 1$ and $T_{i\perp}/T_{i\parallel} < 1$, ion-scale magnetic fluctuations intensify, reaching $\delta B/B_0 \simeq 0.44$ near instability thresholds and regions of high non-bi-Maxwellianity ε_i [Fig. 1(c)]. This suggests that marginally stable and non-bi-Maxwellian iVDFs are associated with large amplitude ion scale magnetic field fluctuations.

To determine if the magnetic field direction is a preferred direction of the ion VDFs, we investigate their alignment with the local magnetic field $\hat{\mathbf{b}}$ [5, 6]. We determine the minimum variance frame (MVF) of the iVDFs by calculating the eigenvalues $\{\lambda_j\}_{j \in [1,3]}$ and the corresponding principal directions $\{\hat{\mathbf{e}}_j\}_{j \in [1,3]}$ of the ion temperature tensor \mathbf{T}_i such that $\lambda_1 \geq \lambda_2 \geq \lambda_3$. We find that the maximum variance direction $\hat{\mathbf{e}}_1$ is predominantly perpendicular to $\hat{\mathbf{b}}$ [Fig. 2(a)]. Meanwhile, the minimum variance direction $\hat{\mathbf{e}}_3$ generally aligns with $\hat{\mathbf{b}}$. Additionally, the eigenvalue ratios are $\lambda_1/\lambda_2 = 1.10^{+0.09}_{-0.05}$ and $\lambda_1/\lambda_3 = 1.30^{+0.33}_{-0.14}$ [Fig. 2(b)]. Given the orientation of $\hat{\mathbf{e}}_1$ and $\hat{\mathbf{e}}_3$ relative to $\hat{\mathbf{b}}$, λ_1/λ_2 indicates agyrotropy, while λ_1/λ_3 represents anisotropy. The λ_1/λ_2 distribution exhibits a distinct non-Gaussian power-law tail with a Pearson kurtosis of $\mu_4 \simeq 77$. However, in some cases, $\hat{\mathbf{e}}_1$ closely aligns with the magnetic field ($|\hat{\mathbf{e}}_1 \cdot \hat{\mathbf{b}}| > 0.8$), coinciding with $\lambda_1/\lambda_2 \simeq 1.15^{+0.15}_{-0.08}$ and $\lambda_1/\lambda_3 \simeq 1.26^{+0.19}_{-0.11}$ (not shown), suggesting nearly isotropic iVDFs with $\lambda_1 \sim \lambda_2 \sim \lambda_3$. These findings confirm a broad anisotropy distribution, predominantly with $T_{i\perp} > T_{i\parallel}$, while agyrotropy remains generally small but reaches significant levels in rare extreme cases.

Thus far, we have analyzed the non-LTE features of the iVDFs without considering turbulence effects. However, numerical simulations suggest that turbulence levels and the mean plasma beta significantly influence deviations from LTE [39]. To explore this dependence, we bin our dataset based on the turbulence level, quantified by the variability of the magnetic field, B_{rms}/B_0 ,

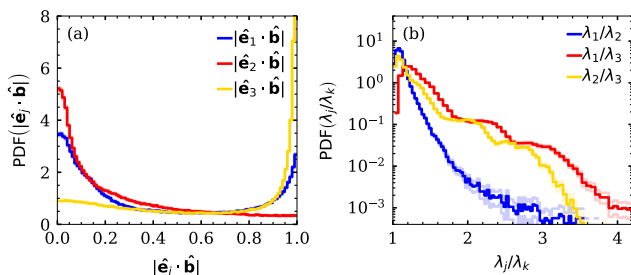


FIG. 2. Non-Maxwellianity of iVDF in the Minimum Variance Frame. (a) PDF of the principal directions $\hat{\mathbf{e}}_i$ relative to the local magnetic field $\hat{\mathbf{b}}$. (b) PDF of the eigenvalue ratio of the iVDFs. Shaded regions represent standard deviations assuming Poisson-distributed statistics [37].

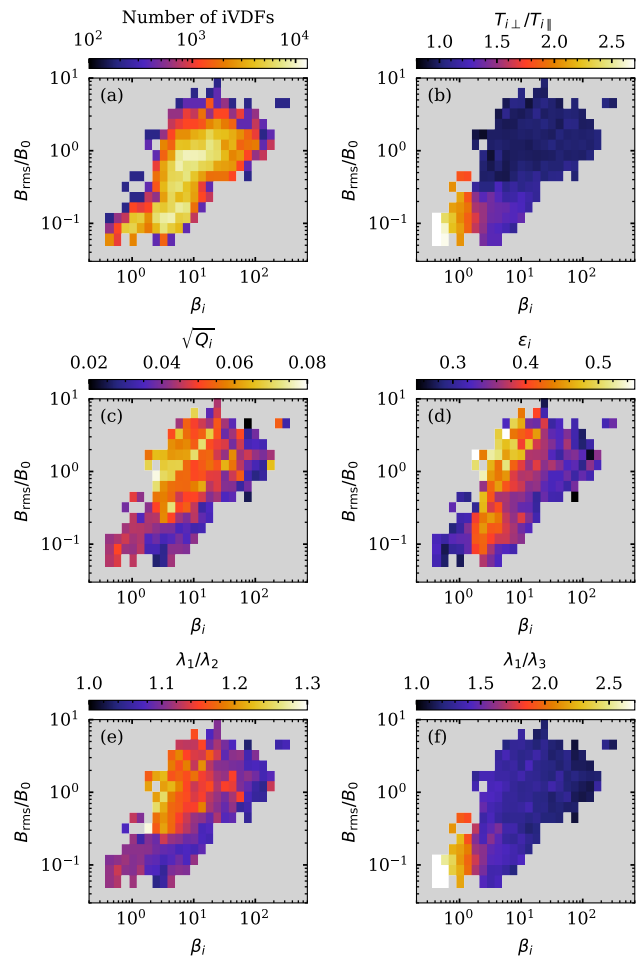


FIG. 3. Conditional averages of the non-Maxwellianity of the iVDFs in the $(\beta_i, B_{\text{rms}}/B_0)$ space. (a) Number of iVDFs. (b) Temperature anisotropy $T_{i\perp}/T_{i\parallel}$. (c) Agyrotropy $\sqrt{Q_i}$. (d) Non-bi-Maxwellianity ε_i . (e) Maximum to intermediate λ_1/λ_2 and (f) maximum to minimum λ_1/λ_3 eigenvalue ratios, respectively.

and the ion plasma parameter, β_i [Fig. 3(a)], where $B_{\text{rms}} = \sqrt{\langle |\mathbf{B} - \mathbf{B}_0|^2 \rangle_{30\text{s}}}$ is the root mean square magnetic fluctuations. We then compute the conditional average of the non-Maxwellianity measures $T_{i\perp}/T_{i\parallel}$, $\sqrt{Q_i}$, ε_i , λ_1/λ_2 , and λ_1/λ_3 in the $(\beta_i, B_{\text{rms}}/B_0)$ space based on the averaged quantities within each 30-second window.

This classification reveals two distinct clusters at $(\beta_i \sim 1, B_{\text{rms}}/B_0 \sim 0.1)$ and $(\beta_i \sim 10, B_{\text{rms}}/B_0 \sim 1)$, indicating a strong correlation between turbulence levels and ion plasma beta. These clusters correspond to the quasi-perpendicular and quasi-parallel magnetosheath, respectively, as demonstrated by Ref. [29]. We find that the temperature anisotropy, $T_{i\perp}/T_{i\parallel}$, decreases with increasing β_i and B_{rms}/B_0 [Fig. 3(b)]. However, due to the correlation between β_i and B_{rms}/B_0 , and the lack of data at $(\beta_i \sim 1, B_{\text{rms}}/B_0 \sim 1)$ and $(\beta_i \sim 10, B_{\text{rms}}/B_0 \sim 0.1)$, it remains unclear whether this decrease is a direct effect of

turbulence or an indirect consequence of its relationship with β_i .

In contrast, the agyrotropy $\sqrt{Q_i}$ [Fig. 3(c)] and the non-bi-Maxwellianity ε_i decrease with β_i but increase with B_{rms}/B_0 [Fig. 3(c), 3(d)]. Notably, at $\beta_i \sim 5$, $B_{\text{rms}}/B_0 \sim 1$, we find values reaching $\sqrt{Q_i} \simeq 0.07$ and $\varepsilon_i \simeq 0.5$, which exceed the dataset mean by one standard deviation ($\sqrt{Q_i} = 0.04_{-0.02}^{+0.02}$, $\varepsilon_i = 0.36_{-0.07}^{+0.11}$) [Figs. 1(b), 1(c)]. Furthermore, the eigenvalue ratios λ_1/λ_2 and λ_1/λ_3 closely follow the trends of agyrotropy and anisotropy, respectively [Figs. 3(b), 3(c), 3(e), 3(f)]. This indicates that in the low- β_i , weakly turbulent regime, iVDFs are compressed along the magnetic field, i.e., $\lambda_1/\lambda_3 > 1$, with little high-order non-Maxwellianity. In contrast, in the high- β_i , strongly turbulent regime, the iVDFs become nearly isotropic with pronounced high-order non-Maxwellian features.

To understand how iVDFs relax toward LTE, we examine the magnetic field curvature relative to the ion scale. In addition to wave-particle interactions, ion scattering in strongly curved magnetic fields can efficiently isotropize iVDFs [5, 22, 40]. We compute the magnetic field curvature $\mathbf{K} = \hat{\mathbf{b}} \cdot \nabla \hat{\mathbf{b}}$ using the multi-spacecraft curlometer technique [30]. The PDF of the normalized magnetic curvature $|\mathbf{K}|/|\mathbf{K}|_{\text{rms}}$ follows a double Pareto log-normal distribution [Fig. 4a]. Notably, the distribution peaks at $|\mathbf{K}|^* \simeq 0.14|\mathbf{K}|_{\text{rms}} \simeq 0.02d_i^{-1}$ (red circle), which corresponds to $|\mathbf{K}|^* \sim \lambda_c^{-1}$, with $\lambda_c \sim 10 - 100d_i$ [28]. Moreover, for $|\mathbf{K}| \ll |\mathbf{K}|^*$ and $|\mathbf{K}| \gg |\mathbf{K}|^*$, the distribution follows power-law slopes of 1 and -2.5 , respectively, confirming theoretical predictions and earlier findings [41, 42].

We compute the adiabaticity parameter, $\kappa = \sqrt{r_c/\rho_i}$, where $r_c = 1/|\mathbf{K}|$ is the radius of curvature of the magnetic field, as a proxy for ion motion dynamics [40] [Fig. 4b]. For $\kappa \gg 1$, ion motion is adiabatic, with the magnetic moment μ conserved to an accuracy of $\Delta\mu/\mu \sim \exp(-2\kappa^2/3)$ [40, 43]. At $\kappa \sim 1$, resonance occurs, leading to chaotic ion motion and strong scattering, characterized by $\Delta\mu/\mu \sim 1$ [40, 43]. For $\kappa \ll 1$, the motion is quasi-adiabatic, with the generalized magnetic moment I_z approximately conserved as $\Delta I_z/I_z \sim \kappa$ for compressional and ~ 1 for force-free discontinuities [44, 45]. We find that for 25% of the iVDFs, the Larmor radius satisfies $\kappa \leq 1.8$ (red shaded area), corresponding to $\Delta\mu/\mu \geq 0.1$ (red circle). Since κ is estimated using the thermal ion speed $v_{thi\perp}$, ions with $v_{i\perp} > v_{thi\perp}$ may remain non-adiabatic even when $\kappa \gg 1$. This indicates that a substantial fraction of the ions follow quasi-adiabatic and chaotic orbits, breaking the adiabatic invariant conservation.

The adiabaticity parameter κ decreases with increasing β_i and B_{rms}/B_0 due to its dependence on ion temperature and magnetic field strength [Fig. 4c]. Notably, its variation as a function of β_i and B_{rms}/B_0 closely follows the trend of temperature anisotropy [Figs. 3(b), 3(f)].

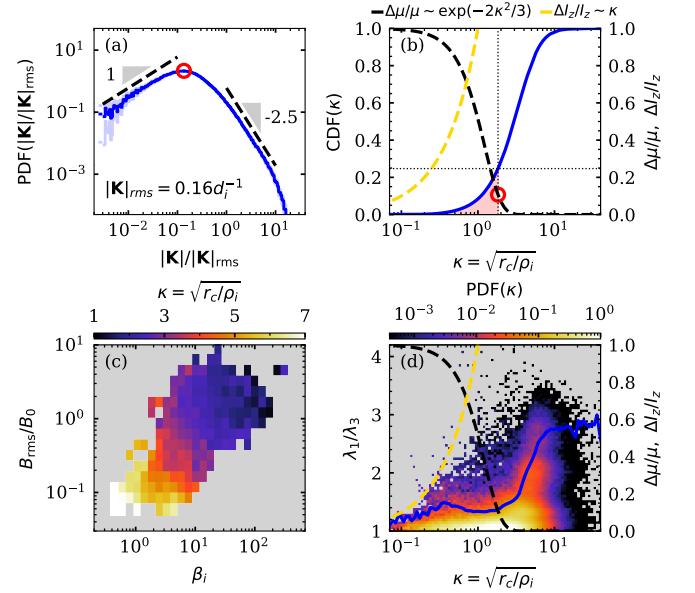


FIG. 4. Magnetic field curvature. (a) PDF of the normalized magnetic field curvature $|\mathbf{K}|/|\mathbf{K}|_{\text{rms}}$, with black dashed lines showing predicted slopes from Ref. [42]. Shaded regions represent standard deviations assuming Poisson-distributed statistics [37]. (b) Cumulative distribution function (CDF) of the adiabaticity parameter κ . (c) Conditional averages of κ in the $(\beta_i, B_{\text{rms}}/B_0)$ space. (d) Joint PDF of the eigenvalue ratio λ_1/λ_3 and κ , with the blue line marking the 95th percentile. The black and gold lines show theoretical jumps $\Delta\mu/\mu$ and $\Delta I_z/I_z$, respectively [40].

Specifically, at $(\beta_i \sim 1, B_{\text{rms}}/B_0 \sim 0.1)$, we find $\kappa \simeq 7$, corresponding to $\Delta\mu/\mu \simeq 2 \times 10^{-16}$, indicating negligible scattering due to magnetic field curvature. In contrast, at $(\beta_i \sim 100, B_{\text{rms}}/B_0 \sim 1)$, $\kappa \sim 1$, leading to $\Delta\mu/\mu \simeq 1$, and ions experience strong scattering. Moreover, κ is strongly correlated with the eigenvalue ratio λ_1/λ_3 [Fig. 4d], with its 95th percentile reaching a minimum at $\kappa \simeq 1.21$, corresponding to $\Delta\mu/\mu \simeq 0.38$, near the expected maximum scattering at $\kappa = 1$. This suggests that the isotropization of iVDFs results from the breakdown of adiabatic invariance due to magnetic field curvature of the order of the ion gyroradius.

Discussion - Our analysis shows that iVDFs in Earth's magnetosheath can deviate significantly from Maxwell-Boltzmann LTE. Many iVDFs are predicted to be unstable to temperature anisotropy-driven instabilities. However, both stable and unstable iVDFs also display notable high-order non-bi-Maxwellian features, suggesting that the bi-Maxwellian model commonly used in linear Vlasov theory may be insufficient to assess the iVDFs' stability [18–20]. Non-LTE iVDFs are often associated with large amplitude magnetic field fluctuations. Interestingly, these fluctuations may be ion scale magnetic shears, pushing the iVDFs further from LTE rather than relaxing them toward marginal stability, as one might

expect from electromagnetic waves [39, 46–48]. Alternatively, these unstable iVDFs may originate at the bow shock and persist across the magnetosheath due to the plasma’s slow transit time across the magnetosheath compared with the relaxation timescales [5].

We demonstrate that the non-Maxwellianity of iVDFs depends on ion plasma beta β_i and turbulence level B_{rms}/B_0 . As B_{rms}/B_0 increases, high-order non-Maxwellian features, including agyrotropy, become more pronounced. This suggests that turbulence drives these higher-order features. Numerical simulations and *in situ* observations support the idea that turbulence-generated current sheets play a key role in creating such features [6–8]. Additionally, the distribution of agyrotropy follows a non-Gaussian power-law tail, which mirrors the behavior of magnetic field increments in turbulence [49, 50]. This further indicates that turbulence is responsible for driving these high-order non-LTE features. Moreover, the fine-scale velocity-space features we measure may be tied to a concurrent phase-space cascade [51], further highlighting the complex interplay between turbulence and iVDF evolution.

Interestingly, despite these high-order non-Maxwellian features, iVDFs in weakly magnetized, highly turbulent regime ($\beta_i \gg 1$, $B_{\text{rms}}/B_0 \sim 1$) tend to be nearly isotropic. In these conditions, magnetic curvature induced by turbulence can be of the order of the thermal ion gyroradius scale or smaller. As a result, ions interact with these turbulence-generated curved magnetic fields, following chaotic orbits and undergoing pitch-angle scattering [22, 40, 43, 52, 53]. Numerical simulations further suggest that such strongly curved magnetic fields enhance particle transport and diffusion [54–56]. This indicates that turbulence distorts magnetic fields across all scales down to sub-ion scales, leading to phase-space diffusion and ion energization as ions interact with these curved fields.

Conclusion - We present the first statistical quantitative analysis of the non-Maxwellianity of iVDFs in the turbulent collisionless plasma in the Earth’s magnetosheath. Our results indicate that the shocked plasma rapidly relaxes. We show that the complexity of non-LTE iVDFs depends on the ion plasma beta and turbulence intensity. As magnetic field fluctuations increase, iVDFs exhibit substantial high-order deviations from LTE, while wave excitation and curvature scattering limit low-order non-LTE. These results highlight the role of turbulence in plasma heating and driving and regulating non-LTE behaviors in iVDFs, providing insights into its interaction with ion velocity distributions in collisionless plasmas.

Acknowledgments - We thank the MMS team for data access and support. L.R. acknowledges support from the Knut and Alice Wallenberg Foundation (Dnr.

2022.0087), the Swedish National Space Agency grant 192/20, and the Royal Swedish Academy of Sciences grant AST2024-0015. S.S. acknowledges the Space It Up project funded by the Italian Space Agency, ASI, and the Ministry of University and Research, MUR, under contract n. 2024-5-E.0 - CUP n. I53D24000060005. I.S. acknowledges support from the Swedish Research Council Grant 2016-0550 and the Swedish National Space Agency Grant 158/16. A.C. acknowledges support from NASA Grants 80NSSC21K0454, 80NSSC22K0688, and 80NSSC24K0172. O.P. acknowledges the project ”2022KL38BK - The ULtimate fate of TuRbulence from space to laboratory plAsmas (ULTRA)” (Master CUP B53D23004850006), by the Italian Ministry of University and Research, funded under the National Recovery and Resilience Plan (NRRP), Mission 4 – Component C2 – Investment 1.1, ”Fondo per il Programma Nazionale di Ricerca e Progetti di Rilevante Interesse Nazionale (PRIN 2022)” (PE9) by the European Union – NextGenerationEU. This research was supported by the International Space Science Institute (ISSI) in Bern through the ISSI International Team project #23-588 (”Unveiling Energy Conversion and Dissipation in Non-Equilibrium Space Plasmas”). L.R. thanks Yu. V. Khotyaintsev for helpful suggestions. Data analysis used the pyrifu analysis package [57].

* louis.richard@ifru.se

- [1] A. A. Schekochihin, S. C. Cowley, W. Dorland, G. W. Hammett, G. G. Howes, E. Quataert, and T. Tatsuno, *Astrophys. J. Suppl. Ser.* **182**, 310 (2009).
- [2] D. Verscharen, K. G. Klein, and B. A. Maruca, *Living Rev. Solar Phys.* **16**, 5 (2019).
- [3] N. A. Krall and A. W. Trivelpiece, *Principles of Plasma Physics* (McGraw-Hill, 1973).
- [4] S. Zenitani, I. Shinohara, T. Nagai, and T. Wada, *Phys. Plasmas* **20**, 092120 (2013).
- [5] L. Richard, Y. V. Khotyaintsev, D. B. Graham, A. Vaivads, D. J. Gershman, and C. T. Russell, *Phys. Rev. Lett.* **131**, 115201 (2023).
- [6] S. Servidio, F. Valentini, F. Califano, and P. Veltri, *Phys. Rev. Lett.* **108**, 045001 (2012).
- [7] A. Greco, F. Valentini, S. Servidio, and W. H. Matthaeus, *Phys. Rev. E* **86**, 066405 (2012).
- [8] S. Perri, D. Perrone, E. Yordanova, L. Sorriso-Valvo, W. R. Paterson, D. J. Gershman, B. L. Giles, C. J. Pollock, J. C. Dorelli, L. A. Avanov, B. Lavraud, Y. Saito, R. Nakamura, D. Fischer, W. Baumjohann, F. Plaschke, Y. Narita, W. Magnes, C. T. Russell, R. J. Strangeway, O. L. Contel, Y. Khotyaintsev, and F. Valentini, *J. Plasma Phys.* **86**, 905860108 (2020).
- [9] V. Zhdankin, *Phys. Rev. X* **12**, 031011 (2022).
- [10] L. Sorriso-Valvo, F. Catapano, A. Retinò, O. Le Contel, D. Perrone, O. W. Roberts, J. T. Coburn, V. Panebianco, F. Valentini, S. Perri, A. Greco, F. Malara, V. Carbone, P. Veltri, O. Pezzi, F. Fraternali, F. Di Mare, R. Marino, B. Giles, T. E. Moore, C. T. Russell, R. B. Torbert, J. L.

- Burch, and Y. V. Khotyaintsev, *Phys. Rev. Lett.* **122**, 035102 (2019).
- [11] G. K. Parks, E. Lee, M. McCarthy, M. Goldstein, S. Y. Fu, J. B. Cao, P. Canu, N. Lin, M. Wilber, I. Dandouras, H. Réme, and A. Fazakerley, *Phys. Rev. Lett.* **108**, 061102 (2012).
- [12] O. V. Agapitov, V. Krasnoselskikh, M. Balikhin, J. W. Bonnell, F. S. Mozer, and L. Avano, *Astrophys. J.* **952**, 154 (2023).
- [13] S. D. Bale, J. C. Kasper, G. G. Howes, E. Quataert, C. Salem, and D. Sundkvist, *Phys. Rev. Lett.* **103**, 211101 (2009).
- [14] T. A. Bowen, B. D. G. Chandran, J. Squire, S. D. Bale, D. Duan, K. G. Klein, D. Larson, A. Mallet, M. D. McManus, R. Meyrand, J. L. Verniero, and L. D. Woodham, *Phys. Rev. Lett.* **129**, 165101 (2022).
- [15] M. D. McManus, K. G. Klein, S. D. Bale, T. A. Bowen, J. Huang, D. Larson, R. Livi, A. Rahmati, O. Romeo, J. Verniero, and P. Whittlesey, *Astrophys. J.* **961**, 142 (2024).
- [16] P. A. Cassak, M. H. Barbhuiya, H. Liang, and M. R. Argall, *Phys. Rev. Lett.* **130**, 085201 (2023).
- [17] B. A. Maruca, A. Chasapis, S. P. Gary, R. Bandyopadhyay, R. Chhiber, T. N. Parashar, W. H. Matthaeus, M. A. Shay, J. L. Burch, T. E. Moore, C. J. Pollock, B. J. Giles, W. R. Paterson, J. Dorelli, D. J. Gershman, R. B. Torbert, C. T. Russell, and R. J. Strangeway, *Astrophys. J.* **866**, 25 (2018).
- [18] K. G. Klein, B. L. Alterman, M. L. Stevens, D. Vech, and J. C. Kasper, *Phys. Rev. Lett.* **120**, 205102 (2018).
- [19] M. M. Martinović, K. G. Klein, T. Āurovcová, and B. L. Alterman, *Astrophys. J.* **923**, 116 (2021).
- [20] M. M. Martinović and K. G. Klein, *Astrophys. J.* **952**, 14 (2023).
- [21] W. H. Matthaeus, S. Oughton, K. T. Osman, S. Servidio, M. Wan, S. P. Gary, M. A. Shay, F. Valentini, V. Roytershteyn, H. Karimabadi, and S. C. Chapman, *Astrophys. J.* **790**, 155 (2014).
- [22] A. V. Artemyev, A. I. Neishtadt, A. A. Vasiliev, V. Angelopoulos, A. A. Vinogradov, and L. M. Zelenyi, *Phys. Rev. E* **102**, 033201 (2020).
- [23] C. C. Chaston, P. Travnicek, and C. T. Russell, *Geophys. Res. Lett.* **47**, e2020GL089613 (2020).
- [24] C. C. Chaston and P. Travnicek, *Geophys. Res. Lett.* **48**, e2021GL094029 (2021).
- [25] A. Retinò, D. Sundkvist, A. Vaivads, F. Mozer, M. André, and C. J. Owen, *Nature Phys* **3**, 235 (2007).
- [26] E. Yordanova, Z. Vörös, A. Varsani, D. B. Graham, C. Norgren, Yu. V. Khotyaintsev, A. Vaivads, E. Eriksson, R. Nakamura, P.-A. Lindqvist, G. Marklund, R. E. Ergun, W. Magnes, W. Baumjohann, D. Fischer, F. Plaschke, Y. Narita, C. T. Russell, R. J. Strangeway, O. Le Contel, C. Pollock, R. B. Torbert, B. J. Giles, J. L. Burch, L. A. Avano, J. C. Dorelli, D. J. Gershman, W. R. Paterson, B. Lavraud, and Y. Saito, *Geophys. Res. Lett.* **43**, 5969 (2016).
- [27] Z. Vörös, E. Yordanova, A. Varsani, K. J. Genestreti, Yu. V. Khotyaintsev, W. Li, D. B. Graham, C. Norgren, R. Nakamura, Y. Narita, F. Plaschke, W. Magnes, W. Baumjohann, D. Fischer, A. Vaivads, E. Eriksson, P.-A. Lindqvist, G. Marklund, R. E. Ergun, M. Leitner, M. P. Leubner, R. J. Strangeway, O. Le Contel, C. Pollock, B. J. Giles, R. B. Torbert, J. L. Burch, L. A. Avano, J. C. Dorelli, D. J. Gershman, W. R. Paterson, B. Lavraud, and Y. Saito, *J. Geophys. Res.* **122**, 11,442 (2017).
- [28] J. E. Stawarz, J. P. Eastwood, T. D. Phan, I. L. Gingell, P. S. Pyakurel, M. A. Shay, S. L. Robertson, C. T. Russell, and O. Le Contel, *Phys. Plasmas* **29**, 012302 (2022).
- [29] I. Svenningsson, E. Yordanova, Y. V. Khotyaintsev, M. André, and G. Cozzani, *J. Geophys. Res.* **130**, e2024JA033272 (2025).
- [30] P. Robert, M. W. Dunlop, A. Roux, and G. Chanteur, in *Analysis Methods for Multi-Spacecraft Data*, Vol. 1, edited by G. Paschmann and P. W. Daly (1998) pp. 395–418.
- [31] C. T. Russell, B. J. Anderson, W. Baumjohann, K. R. Bromund, D. Dearborn, D. Fischer, G. Le, H. K. Leinweber, D. Leneman, W. Magnes, J. D. Means, M. B. Moldwin, R. Nakamura, D. Pierce, F. Plaschke, K. M. Rowe, J. A. Slavin, R. J. Strangeway, R. Torbert, C. Hagen, I. Jernej, A. Valavanoglou, and I. Richter, *Space Sci. Rev.* **199**, 189 (2016).
- [32] C. Pollock, T. Moore, A. Jacques, J. Burch, U. Gliese, Y. Saito, T. Omoto, L. Avano, A. Barrie, V. Coffey, J. Dorelli, D. Gershman, B. Giles, T. Rosnack, C. Salo, S. Yokota, M. Adrian, C. Aoustin, C. Aulletti, S. Aung, V. Bigio, N. Cao, M. Chandler, D. Chornay, K. Christian, G. Clark, G. Collinson, T. Corris, A. De Los Santos, R. Devlin, T. Diaz, T. Dickerson, C. Dickson, A. Diekmann, F. Diggs, C. Duncan, A. Figueroa-Vinas, C. Firman, M. Freeman, N. Galassi, K. Garcia, G. Goodhart, D. Guererro, J. Hageman, J. Hanley, E. Hemminger, M. Holland, M. Hutchins, T. James, W. Jones, S. Kreisler, J. Kujawski, V. Lavu, J. Lobell, E. LeCompte, A. Lukemire, E. MacDonald, A. Mariano, T. Mukai, K. Narayanan, Q. Nguyen, M. Onizuka, W. Paterson, S. Persyn, B. Piepgrass, F. Cheney, A. Rager, T. Raghuram, A. Ramil, L. Reichenthal, H. Rodriguez, J. Rouzaud, A. Rucker, Y. Saito, M. Samara, J.-A. Sauvaud, D. Schuster, M. Shappirio, K. Shelton, D. Sher, D. Smith, K. Smith, S. Smith, D. Steinfeld, R. Szymkiewicz, K. Tanimoto, J. Taylor, C. Tucker, K. Tull, A. Uhl, J. Vloet, P. Walpole, S. Weidner, D. White, G. Winkert, P.-S. Yeh, and M. Zeuch, *Space Sci. Rev.* **199**, 331 (2016).
- [33] D. J. Gershman, J. C. Dorelli, L. A. Avano, U. Gliese, A. Barrie, C. Schiff, D. E. Da Silva, W. R. Paterson, B. L. Giles, and C. J. Pollock, *J. Geophys. Res.* **124**, 10345 (2019).
- [34] M. Swisdak, *Geophys. Res. Lett.* **43**, 43 (2016).
- [35] T. Motoba, M. I. Sitnov, G. K. Stephens, and D. J. Gershman, *J. Geophys. Res.* **127**, e2022JA030514 (2022).
- [36] D. Verscharen, B. D. G. Chandran, K. G. Klein, and E. Quataert, *Astrophys. J.* **831**, 128 (2016).
- [37] R. Barlow, *Statistics. A Guide to the Use of Statistical Methods in the Physical Sciences* (The Manchester Physics Series, 1989).
- [38] D. B. Graham, Y. V. Khotyaintsev, M. André, A. Vaivads, A. Chasapis, W. H. Matthaeus, A. Retinò, F. Valentini, and D. J. Gershman, *J. Geophys. Res.* **126**, e2021JA029260 (2021).
- [39] S. Servidio, K. T. Osman, F. Valentini, D. Perrone, F. Califano, S. Chapman, W. H. Matthaeus, and P. Veltri, *Astrophys. J. Lett.* **781**, L27 (2014).
- [40] J. Büchner and L. M. Zelenyi, *J. Geophys. Res.* **94**, 11821 (1989).
- [41] Y. Yang, M. Wan, W. H. Matthaeus, Y. Shi, T. N.

- Parashar, Q. Lu, and S. Chen, *Phys. Plasmas* **26**, 072306 (2019).
- [42] R. Bandyopadhyay, Y. Yang, W. H. Matthaeus, A. Chasapis, T. N. Parashar, C. T. Russell, R. J. Strangeway, R. B. Torbert, B. L. Giles, D. J. Gershman, C. J. Pollock, T. E. Moore, and J. L. Burch, *Astrophys. J. Lett.* **893**, L25 (2020).
- [43] T. J. Birmingham, *J. Geophys. Res.* **89**, 2699 (1984).
- [44] G. R. Burkhart, P. B. Dusenbery, and T. W. Speiser, *J. Geophys. Res.* **100**, 107 (1995).
- [45] A. V. Artemyev, A. I. Neishtadt, and L. M. Zelenyi, *Phys. Rev. E* **89**, 060902 (2014).
- [46] K. T. Osman, W. H. Matthaeus, B. Hnat, and S. C. Chapman, *Phys. Rev. Lett.* **108**, 261103 (2012).
- [47] M. W. Kunz, A. A. Schekochihin, and J. M. Stone, *Phys. Rev. Lett.* **112**, 205003 (2014).
- [48] D. Del Sarto, F. Pegoraro, and F. Califano, *Phys. Rev. E* **93**, 053203 (2016).
- [49] D. Sundkvist, A. Retinò, A. Vaivads, and S. D. Bale, *Phys. Rev. Lett.* **99**, 025004 (2007).
- [50] E. Yordanova, A. Vaivads, M. André, S. C. Buchert, and Z. Vörös, *Phys. Rev. Lett.* **100**, 205003 (2008).
- [51] S. Servidio, A. Chasapis, W. H. Matthaeus, D. Perrone, F. Valentini, T. N. Parashar, P. Veltri, D. Gershman, C. T. Russell, B. Giles, S. A. Fuselier, T. D. Phan, and J. Burch, *Phys. Rev. Lett.* **119**, 205101 (2017).
- [52] A. V. Artemyev, D. L. Vainchtein, A. I. Neishtadt, and L. M. Zelenyi, *Phys. Rev. E* **93**, 053207 (2016).
- [53] F. Malara, S. Perri, and G. Zimbardo, *Phys. Rev. E* **104**, 025208 (2021).
- [54] S. Servidio, C. T. Haynes, W. H. Matthaeus, D. Burgess, V. Carbone, and P. Veltri, *Phys. Rev. Lett.* **117**, 095101 (2016).
- [55] M. Lemoine, *Phys. Rev. Lett.* **129**, 215101 (2022).
- [56] M. Lemoine, *J. Plasma Phys.* **89**, 175890501 (2023).
- [57] See <https://pypi.org/project/pyrfu/>.